Insightful Closed-Form Expressions for Small-Signal S-Parameters of BJTs

AHMED E NADEEM
Department of Avionics Engineering
College of Aeronautical Engineering
National University of Sciences & Technology
Risalpur, District Nowshera, NWFP
PAKISTAN

WILLIAM R EISENSTADT
Department of Electrical & Computer Engineering
University of Florida
Gainesville, FL 32611
USA

Abstract: - A relationship between small-signal s-parameters and equivalent circuit model for BJTs is presented in this paper. Closed-form expressions for small-signal s-parameters of BJTs derived using intrinsic high-frequency hybrid-π model have been verified against on-wafer measurements from 45 MHz to 20.045 GHz. Excellent agreement between the measurements and s-parameters calculated using closed-form expressions has been shown over the entire frequency range. A comparison of s-parameters measured, calculated using closed-form expressions, and obtained through HP-MDS simulation is also presented in this paper.

Key-Words: - Closed-form expressions for S-parameters of BJTs

1 Introduction

In the 1970s, with the advancements in RF and Microwave measurement equipment, mainly the network analyzers and on-wafer probes, the popularity and applications of s-parameters increased tremendously. Now, RF and microwave circuit design methodologies are centered around the s-parameter data of active and passive devices.

Today, RF/microwave planar circuits have found applications in the fields of communications, electronic warfare, radars, and weapon systems. Among many environmental variables, temperature is the most obvious one that neither remains the same in different applications, nor remains constant in any one system. Virtually, every transistor parameter is directly or indirectly affected by temperature because of thermal dependence of the physical properties of the materials used to fabricate semiconductor devices. Therefore, the electrical properties (currents and voltages) of a device are also temperature dependent. This broad thermal dependence of device parameters implies that s-parameters must also be temperature dependent. Forward transmission gain (S_{21}) is well known to be a strong function of collector current in BJTs which itself is quite sensitive to temperature [1,2]. It has also been shown that not only all four s-parameters (S_{11}, S_{21}, S_{12}, and S_{22}) are bias sensitive, but their magnitudes and phases also vary due to change in temperature even when constant collector current is maintained [3]. This implies that besides bias current there are other factors as well that cause variations in s-parameters.

S-parameters of an active or a passive device are defined and also measured as the ratios of the incident and reflected power waves of n-port network. These incident and reflected power waves are related to the external voltages and currents at each port of the network. Therefore, s-parameter characterization is limited to the external voltages and currents at each of the two ports of the network representing the device. Measurement data is the most reliable means to quantify the dependence of s-parameters on temperature sensitive quantities such as bias current, etc., but the nature of the measurements is external to the network. Thus direct measurements tend to limit or completely obscure the insight to the device behavior, which in fact causes the variations in s-parameters with temperature. Computer simulations; when used to quantify the sensitivity of s-parameters at different bias conditions or temperatures tend to mask device

behavior as well. To perform design-oriented sensitivity analysis of s-parameters, it is necessary to (a) gain an insight into the network itself to identify the sources which cause variations, and (b) describe them both quantitatively and qualitatively. To realize these objectives, s-parameters of a transistor need to be linked with the device model parameters. As regards to the relationship between s-parameters and device model parameters, the only references found are in the context of feedback effects on broadband amplifier design [4,5]. The prior work was neither focused on closed-form expressions for s-parameters nor intended to develop insightful relationships between s-parameters of a BJT and its high-frequency equivalent circuit model. Also, the work by Gonzalez [4] is based on overly simplified low-frequency negative feedback model for BJTs. Hence, the work reported in this paper is the original work.

2 Expressions for S-Parameters

To derive the relationship between small-signal s-parameters and the device model parameters, the intrinsic high frequency hybrid-π model shown in Fig. 1 has been used. The underlying motivation for using hybrid-π model to derive the closed-form expressions for small-signal s-parameters is that all its constituents are simple resistors or capacitors whose frequency behavior is well known except controlled source ($g_m v_{be}$). Also, the hybrid-π model represents the BJT from DC to higher frequencies, so long as the base transit time (τ_B) is much smaller than the signal time period (T) [6]. At higher frequencies, the small-signal transconductance (g_m) become complex [7]. However, during this work a real value for g_m has been used. This was considered sufficient because for all the active devices used, the frequency f_a (the frequency up to which g_m is practically equal to g_{m0} with only a very small phase angle) was found to be several orders of magnitude higher than the frequency of interest.

To develop the two-port representation in terms of the intrinsic device parameters, a matrix analysis of the high-frequency equivalent circuit shown in Fig. 1 is essential. To express s-parameters in terms of device model parameters, the indefinite admittance matrix approach was employed [8]. To proceed, an equivalent circuit in terms of admittances is drawn along with the current sources connected to each node as shown in Fig. 2. A system of nodal equations for the voltages between nodes 1 to 6 and an external reference node indicated as a common node are written.

$$i_1 = y_b V_1 - y_b V_2 \quad (1)$$

$$i_2 = -y_b V_1 + (y_b + y_\delta + y_i) V_2 - y_\delta V_3 - y_i V_5 \quad (2)$$

$$i_3 = -(y_\delta + g_m) V_2 + (y_\delta + y_e + y_o + g_m) V_3 - y_e V_4 - y_o V_5 \quad (3)$$

$$i_4 = -y_e V_3 + y_e V_4 \quad (4)$$

$$i_5 = (g_m - y_i) V_2 - (y_o + g_m) V_3 + (y_i + y_o + y_c) V_5 - y_c V_6 \quad (5)$$

$$i_6 = -y_c V_5 + y_c V_6 \quad (6)$$

This results in a 6x6 matrix. Nodes 2, 3, and 5 are completely inaccessible. These nodes are mathematically removed from the above equations by eliminating the current source i_2, solving for V_2 in terms of the other node voltages, and substituting the result back into the nodal equations having V_2 term. The expression for V_2 after setting $i_2 = 0$ becomes

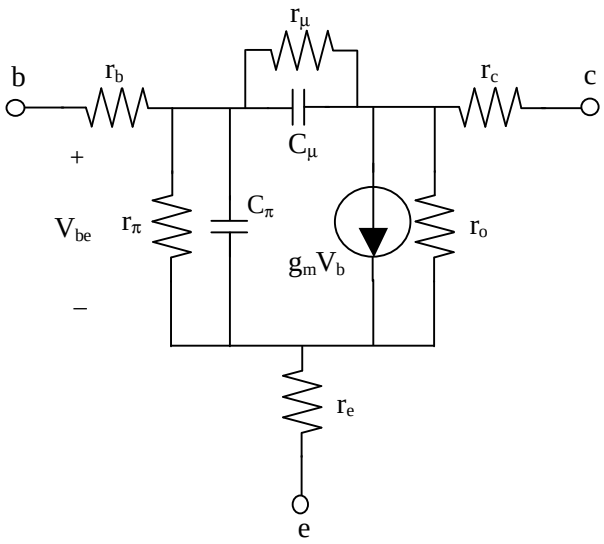

Fig. 1. Intrinsic high-frequency hybrid-π model.

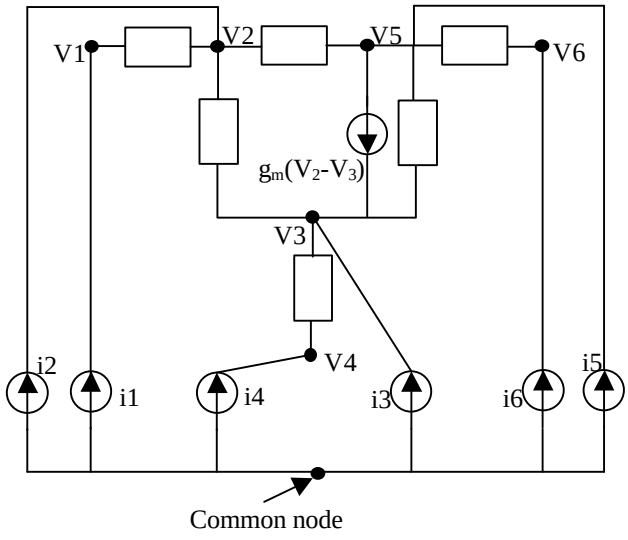

Fig. 2. Equivalent circuit for indefinite admittance matrix.

$$V_2 = \frac{y_b V_1 + y_\delta V_3 + y_\iota V_5}{y_b + y_\delta + y_\iota} \quad (7)$$

This expression for V_2 is substituted in Eq. (1), (3) and (5). After these equations are updated they become independent of V_2. This procedure is repeated for other two nodes i.e. 3 and 5 and eventually the resulting matrix is a 3x3-admittance matrix. This 3x3 matrix does not have any term corresponding to inaccessible nodes, however, the effects have been accounted for. Using the property of the indefinite matrix, node 4 is eliminated for common emitter configuration, and the result is a 2x2-admittance matrix. The elements of the matrix or y-parameters are then normalized with respect to 50 ohms and converted into s-parameters using the standard conversion tables [2, 4, 9-13]. The entire sequence of derivation of small-signal s-parameters in terms of small-signal high-frequency equivalent circuit model parameters is shown in Fig. 3. The conversion and simplification of the expressions was done using MAPLE [14] and hand analysis together. The resulting small-signal s-parameters in terms of equivalent circuit model parameters are as follows:

$$S_{11} = \frac{-CZ_o^2 + ((r_b - r_c)C - r_\iota (Br_o - r_\delta))Z_o + D + E + F}{Denom} \quad (8)$$

$$S_{12} = \frac{2Zo(Cr_e - Ar_\delta r_o)}{Denom} \quad (9)$$

$$S_{21} = \frac{2Z_o(Cr_e + (A - g_m r_\iota) r_\delta r_o)}{Denom} \quad (10)$$

$$S_{22} = \frac{-CZ_o^2 - ((r_b - r_c)C - r_\iota (Br_o - r_\delta))Z_o + D + E + F}{Denom} \quad (12)$$

where

$A = 1 + s\, r_\mu C_\mu$, $B = 1 + s\, r_\pi C_\pi$,

$C = A\, r_\pi (1 + g_m r_o) + B (A\, r_o + r_\mu)$,

$D = (A ((r_c + r_e) r_b + r_e r_c) + r_e r_\mu) r_\pi r_o g_m$,

$E = ((AB (r_c + r_e) B r_\mu + A r_\pi) r_b + (A r_c + r_\mu) (B r_e + r_\pi)) r_o$.

$F = (A r_\pi + B r_\mu)((r_c + r_e) r_b + r_e r_c) + r_\mu r_\pi (r_c + r_e)$, and

$Denom = C Z_o^2 + ((r_b + r_c + 2r_e) C + (A r_o + r_\mu) r_\pi + (A r_\pi + B r_\mu) r_o) Z_o + D + E + F$.

The closed-form expressions derived in this section establish an insightful link between small-signal s-parameters of a BJT and its intrinsic hybrid-π model.

3 Experimental Verification

Before proceeding with experimental verification of closed-form expressions, it is appropriate to state the assumptions used to calculate the small-signal s-parameters using the closed-form expressions derived in the previous section. The numerical values for the small- signal model parameters have been computed using HSPICE by linearizing the static and large signal model parameters for the transistors [15, 16]. The resistances r_b, r_e, and r_c, have been assumed constant for this work and their values have been taken from the model parameters for the transistors used.

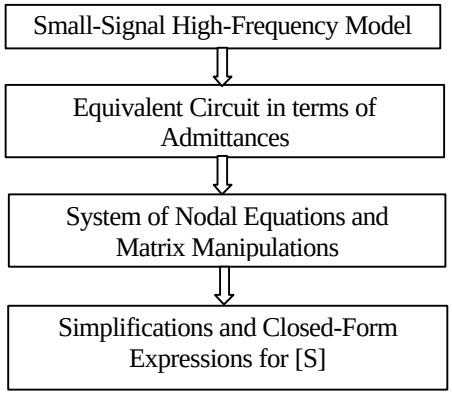

Fig. 3. Sequence of steps for derivation of closed-form expressions for s-parameters of BJTs.

On-wafer s-parameter measurements were done using an Automatic Network Analyzer HP 8510C [17] and coplanar probes over a broad range of frequencies from 45 MHz to 20.045 GHz at room temperature for various devices inside an RF screen room with solid copper walls all around. Prior to device measurements, the network analyzer was duly calibrated using TRL technique and the full two-port error model implemented in HP8510C was employed. The measurement data was corrected using y-parameter de-embedding technique [18].

The comparison of measured and calculated small-signal s-parameters for an npn transistor is given in Fig.4. As shown, the small- signal s-parameters obtained from on-wafer measurements and calculated by using the closed-form expressions have excellent agreement over the entire frequency range. The magnitudes and phase angles for all four s-parameters both measured and calculated except magnitude of S_{22} not only follow the same trend through out the frequency range, but they are very close to each other. The closed-form expressions overestimate the magnitudes of S_{21} and S_{12} by approximately 1.0 and 3.0 dBs respectively, while the phase angles for S_{11} and S_{21} are underestimated by approximately 8 and 10 degrees respectively when compared to measurements. These differences between the measured and calculated s-parameters are at the higher end of the frequency range.

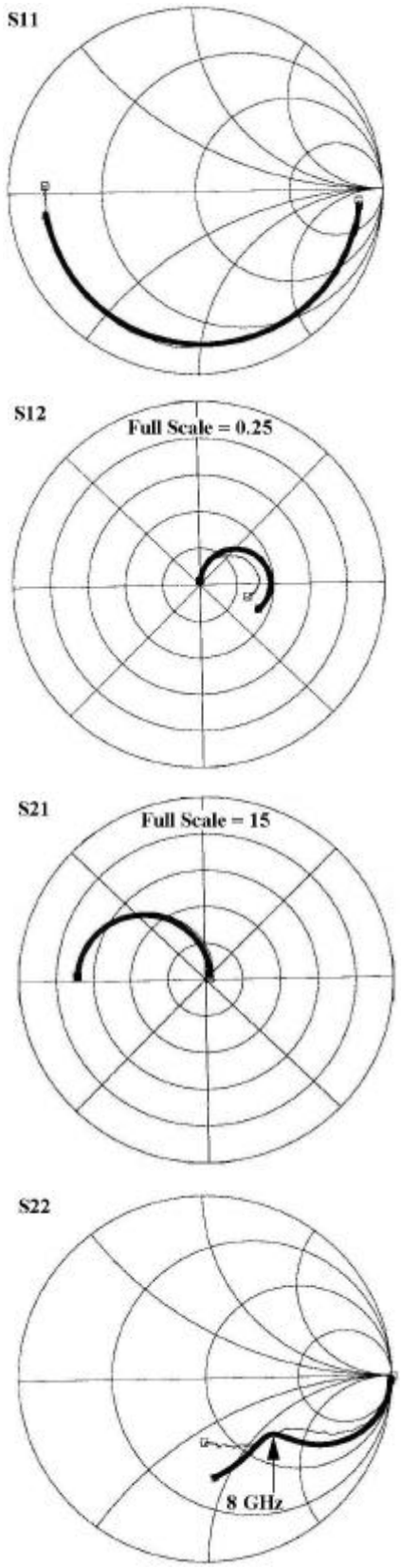

Fig. 4. Comparison of measured (light) and calculated (bold) s-parameters for npn BJT at VCE = 3V and IC = 3mA from 45 MHz to 20.045 GHz.

The small differences between the calculated and measured s-parameters can be attributed to several factors such as; (a) inaccuracies during extraction of device model parameters; (b) process variations during fabrication; (c) assumptions of constant r_b and r_c when they are in fact sensitive to bias conditions; and (d) neglecting capacitance between external base and collector and the substrate effects while deriving small-signal s-parameter expressions.

To gain an insight into the possible cause(s) for the significant difference in measured and calculated output reflection coefficient (S_{22}), the data plotted on impedance (Z) Smith chart in Fig. 4 is further analyzed. As shown, at approximately 8 GHz the magnitude of measured S_{22} starts to depart from the calculated S_{22}, and then shortly after it starts following almost a clockwise path moving towards the upper half of the Smith chart - a signature of series inductance along with reduced capacitive reactance. The departure of measured S_{22} from the calculated S_{22} in magnitude could be attributed to either (a) inductive behavior of collector at higher frequencies, or (b) due to the substrate effects that become significant at higher frequencies. It is worth mentioning here that in addition to collector to substrate capacitance, the substrate contributes both capacitance and substrate resistance. Collector to substrate capacitance in series with substrate resistance appears in parallel with small-signal output resistance (r_o). At higher frequencies when the substrate effect is greater, then the parallel combination of large r_o and relatively smaller collector to substrate capacitance plus a parallel combination of substrate resistance and capacitance may result into smaller output impedance. The effects of substrate have not been included in the derivation of closed-form expressions due to the fact that neither substrate resistance is part of hybrid-π model used during this work, nor the manufacturers as part of device model parameters provide this data. Also, to estimate substrate resistance, detailed information about the layout geometry and dimensions is necessary. Despite neglecting these substrate effects, the deviation of calculated S_{22} from the measured S_{22} in magnitude is less than 1 dB up to 12 GHz and around 3 dB at 20 GHz. As regards to the phase of S_{22} in both cases, there has been an excellent agreement throughout the entire frequency range. Closed-form expressions for small-signal s-parameters have been extensively verified for various transistors under several different bias conditions and the results have been very encouraging.

4 Measured, Calculated, and Simulated S-Parameters

Besides measurements using automatic network analyzers, small-signal s- parameters can also be obtained through computer simulations using HSPICE or HP-MDS [19]. In these circuit simulators, a complete set of device model parameters for the BJT is supplied by the user or accessed from the built in component libraries for active devices. The simulator numerically computes the small-signal model parameters by linearizing the static and large-signal model parameters. These small-signal model parameters are then used for computing the small-signal s-parameters for the user specified frequency range. In both simulation tools, complete device model such as Gummel-Poon in HSPICE or Gummel-Poon or MEXTRAM in HP-MDS is employed for these s-parameter computations. Parasitics elements of the model such as capacitance between external base and collector and collector to substrate capacitance are also included. This section presents a comparison of small-signal s-parameters obtained from (a) on-wafer measurements, (b) closed-form expressions derived during this work, and (c) computer simulations using HP-MDS. The underlying motivation for comparing the small-signal s-parameters obtained from three distinct sources is (a) to determine the relative rank of s-parameters calculated using closed-form expressions, when compared with simulation against measurements, (b) to identify the strengths and weaknesses of the results obtained using closed-form expressions vis-a-vis computer simulations, and (c) to establish the utility, significance, and merits of the closed-form expressions for calculating/predicting small-signal s-parameters of BJT for any bias condition.

A comparison of measured, calculated, and simulated small-signal s-parameters for an npn transistor in common-emitter configuration is presented in Fig. 5. As shown in Fig. 5, for S_{11}, measurements and closed-form predictions are in excellent agreement both in magnitude and phase for the entire frequency range, where as the simulation greatly underestimates the magnitude, while the phase agrees fairly well with measurements. Comparison of reverse transmission coefficient (S_{12}) shows once again good agreement for magnitude and an excellent match of phase of measured and calculated data, while simulation greatly overestimates magnitude and underestimates phase. For S_{21}, measured and calculated data agree well for the entire frequency range, where as simulated S_{21} has much different phase. Simulated S_{22} also exhibits a different trend compared to the measured S_{22}, where as calculated S_{22} displays a deviation from the measurement data only at higher frequencies, while the

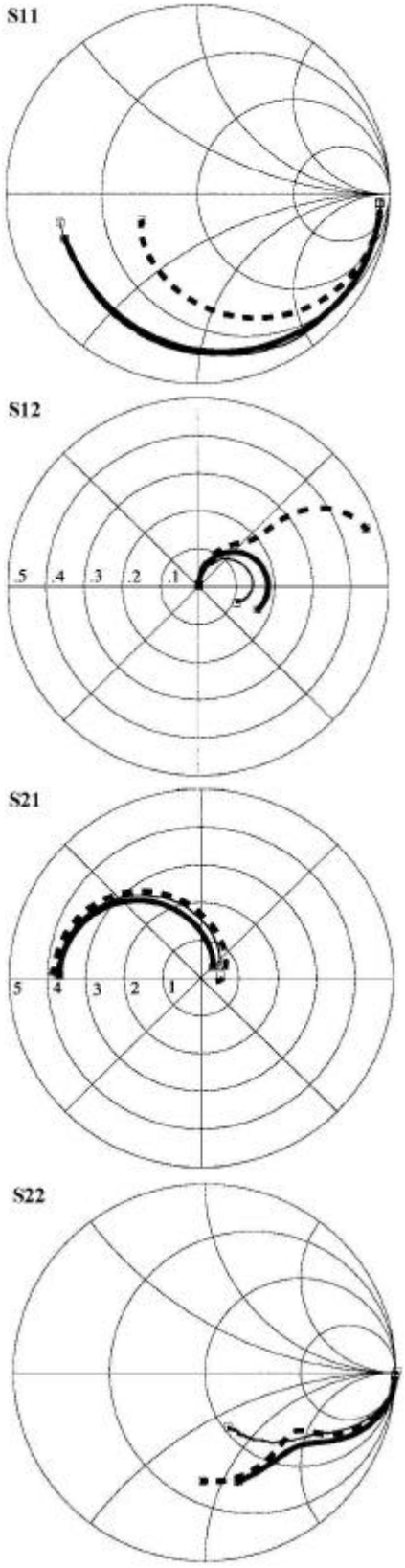

Fig. 5. Comparison of measured (light), calculated (bold), and simulated (dash) s-parameters for npn BJT at VCE = 1V and IC = 1mA from 45 MHz to 20.045 GHz.

phase matches well with measurement. As regards the phase angles of small-signal s-parameters compared, Fig. 5 shows that the calculated data tracks the measurements very well over the entire range of frequencies, where as except for S_{11}, the phase angles of the other three s- parameters i.e. S_{12}, S_{21}, and S_{22}, the difference between measurement and simulation is fairly large. For S_{21}, although the trend seems to be similar to the measurement, but the simulation greatly overestimates the phase. The phase of S_{12} is predicted correctly for only a very narrow frequency range and there after the variation in phase with frequency is significantly different both in values and trend.

5 Conclusion

In this paper, a relationship between small-signal s-parameters and high- frequency equivalent circuit model for BJTs has been presented. Closed-form expressions for two-port s-parameters in a common-emitter configuration have been derived using intrinsic high-frequency hybrid-π model for BJTs. The closed-form expressions have been verified against on-wafer measurements from 45 MHz to 20.045 GHz. Excellent agreement between the s- parameters calculated using closed-form expressions and measured has been shown over the entire frequency range. A comparison between measured, calculated and simulated small-signal s-parameters has been presented. It has been shown that s-parameter calculated using closed-form expressions derived during this work match the measurements more closely compared to s-parameters obtained through HP-MDS simulation.

References:

[1] "Microwave Transistor Bias Considerations," Hewlett-Packard Application Note 944-1, April, 1975.

[2] George D. Vendelin, Anthony M. Pavio, and Ulrich L. Rhode, *Microwave Circuit Design Using Linear and Nonlinear Techniques*, John Wiley & Sons, Inc. 1990.

[3] Ahmed E Nadeem, *Thermal Effects on RF/Microwave Circuit and DC Bias Network Design*, Ph.D Dissertation, University of Florida, Gainesville, 1998.

[4] Guillermo Gonzalez, *Microwave Transistor Amplifier*, Prentice-Hall, Inc., Englewood Cliffs, New Jersey 1984.

[5] William R. Eisenstadt, "Compund Feedback for Bipolar Circuits," Unpublished Notes, 1995.

[6] Ader Bar-Lev, *Semiconductors and Electronic Devices*, 2nd Ed, Prentice-Hall International, 1984.

[7] Aldert Van der Zeil, *Solid State Physical Electronics*, 3rd Edition, Prentice-Hall, Inc. Englewood Cliffs, New Jersey, 1976.

[8] Alfred J. Cote, Jr. and J. Barry Oakes, *Linear Vacuum-Tube and Transistor Circuits*, McGraw-Hill Book Co. Inc., New York, 1961.

[9] R. E. Collin, *Foundations for Microwave Engineering*, McGraw-Hill, New York, 1966.

[10] L. N. Dworsky, *Modern Transmission Line Theory and Applications*, John Wiley & Sons, New York, 1979.

[11] K. C. Gupta, Ramesh Garg and Rakesh Chadha, *Computer-Aided Design of Microwave Circuits*, Artech House, Dedham, Massachusetts, 1981.

[12] George D. Vendelin, *Design of Amplifiers and Oscillators by the S-Parameter Method*, Wiley, New York. 1982.

[13] D. Roddy, *Microwave Technology*, Prentice-Hall, Inc. Englewood Cliffs, New Jersey, 1986.

[14] MAPLE V Release 4, Springer-Verelag, New York, 1996.

[15] *HSPICE User's Manual, Version H92*, Meta-Software, Inc. 1300 White Oaks Road, Campbell, California, 1992.

[16] Giuseppe Massobrio and Paolo Antognetti, *Semiconductor Device Modelling with SPICE*, McGraw-Hill, New York, 1993.

[17] HP 8510C Network Analyzer, Operating and Programming Manual, Hewllet-Packard Company, 1400 Fountaingrove Parkway, Santa Rosa California , 1994.

[18] Paul J. van Wijnen, H. R. Claessen and E. A. Wolsheimer, "A New Straightforward Calibration and Correction Procedure for On-Wafer High-Frequency S-Parameter Measurements (45 MHz-18 GHz)," IEEE 1987 BCTM, pp. 70, 1987

[19] Microwave Design System, Release 7.0, Hewlett-Packard Co., HP Eesof Division, Santa Rosa, California, 1996.